

1 **COVID-19 mRNA third dose induces a unique hybrid immunity-like antibody response**

2 Emanuele Andreano^{1,11}, Ida Paciello^{1,11}, Giulio Pierleoni², Giulia Piccini³, Valentina Abbiento¹, Giada
3 Antonelli¹, Piero Pileri¹, Noemi Manganaro¹, Elisa Pantano¹, Giuseppe Maccari⁴, Silvia Marchese⁵, Lorena
4 Donnici⁶, Linda Benincasa², Ginevra Giglioli², Margherita Leonardi^{2,3}, Concetta De Santi¹, Massimiliano
5 Fabbiani⁷, Ilaria Rancan⁷, Mario Tumbarello^{7,8}, Francesca Montagnani^{7,8}, Claudia Sala¹, Duccio Medini⁴,
6 Raffaele De Francesco^{5,6}, Emanuele Montomoli^{2,3,9}, Rino Rappuoli^{1,10,*}

7

8 ¹Monoclonal Antibody Discovery (MAD) Lab, Fondazione Toscana Life Sciences, Siena, Italy

9 ²VisMederi Research S.r.l., Siena, Italy

10 ³VisMederi S.r.l, Siena, Italy

11 ⁴Data Science for Health (DaScH) Lab, Fondazione Toscana Life Sciences, Siena, Italy

12 ⁵Department of Pharmacological and Biomolecular Sciences DiSFeB, University of Milan, Milan, Italy

13 ⁶INGM, Istituto Nazionale Genetica Molecolare "Romeo ed Enrica Invernizzi", Milan, Italy

14 ⁷Department of Medical Sciences, Infectious and Tropical Diseases Unit, Siena University Hospital, Siena, Italy

15 ⁸Department of Medical Biotechnologies, University of Siena, Siena, Italy

16 ⁹Department of Molecular and Developmental Medicine, University of Siena, Siena, Italy

17 ¹⁰Department of Biotechnology, Chemistry and Pharmacy, University of Siena, Siena, Italy

18 ¹¹These authors contributed equally: Emanuele Andreano, Ida Paciello

19 *Corresponding author: Rino Rappuoli rino.r.rappuoli@gsk.com

20 **ABSTRACT**

21 The continuous evolution of SARS-CoV-2 generated highly mutated variants, like omicron BA.1 and BA.2, able
22 to escape natural and vaccine-induced primary immunity^{1,2}. The administration of a third dose of mRNA
23 vaccines induces a secondary response with increased protection. We investigated, at single-cell level, the
24 longitudinal evolution of the neutralizing antibody response in four donors after three mRNA doses³. A total
25 of 4,100 spike protein specific memory B cells were single cell sorted and 350 neutralizing antibodies were
26 identified. The third dose increased the antibody neutralization potency and breadth against all SARS-CoV-2
27 variants of concern as previously observed with hybrid immunity³. However, the B cell repertoire that stands
28 behind the response is dramatically different. The increased neutralizing response was largely due to the
29 expansion of B cell germlines poorly represented after two doses, and the reduction of germlines
30 predominant after primary immunization such as IGHV3-53;IGHJ6-1 and IGHV3-66;IGHJ4-1. Divergently to
31 hybrid immunity, cross-protection after a third dose was mainly guided by Class 1/2 antibodies encoded by
32 IGHV1-58;IGHJ3-1 and IGHV1-69;IGHJ4-1 germlines. The IGHV2-5;IGHJ3-1 germline, which induced broadly
33 cross-reactive Class 3 antibodies after infection or viral vector vaccination, was not induced by a third mRNA
34 dose. Our data show that while neutralizing breadth and potency can be improved by different immunization
35 regimens, each of them has a unique molecular signature which should be considered while designing novel
36 vaccines and immunization strategies.

37 **INTRODUCTION**

38 The emergence of SARS-CoV-2 variants of concern (VoCs) able to escape vaccine immunity elicited by the
39 spike (S) protein of the original virus isolated in Wuhan, China, have decreased the impact of vaccination^{4,5}.
40 As a consequence, the COVID-19 pandemic continues to impact the health, the economy and the freedom
41 of people worldwide in spite of the several billion doses of vaccines already deployed. This scenario raises
42 new important questions about the use of the existing vaccines and the immunity they can provide to tackle
43 current and future variants. Therefore, it became of utmost importance to understand the nature and the
44 quality of the immune response elicited by the different vaccines used worldwide. In our previous study we
45 analyzed at single cell level the immune response induced by two doses of the BNT162b2 mRNA vaccine in
46 naïve people and in people that had been previously infected by the SARS-CoV-2 virus³. In this study we
47 analyzed at single cell level the longitudinal B cell and neutralizing antibody response of the same naïve
48 people after a third immunization. We found that, while the overall immune response after a third dose is
49 similar to that observed in the hybrid immunity of vaccinated people previously infected by the virus, the B
50 cell repertoire that stands behind the response is dramatically different.

51

52 **RESULTS**

53 **B cells response after third dose**

54 To evaluate the longitudinal evolution of the neutralizing antibody response, four seronegative donors that
55 participated in our previous study after two doses of BNT162b2 mRNA vaccine³, were re-enrolled after
56 receiving a third dose. None of the subjects were exposed to SARS-CoV-2 infection between the second and
57 third vaccination dose. Data after the third dose (seronegative 3rd dose; SN3) described in this study were
58 compared to those obtained from the same subjects after the second dose (seronegative 2nd dose; SN2) and
59 to those of subjects with hybrid immunity (seropositive 2nd dose; SP2) previously described³. Three subjects
60 received the BNT162b2 (VAC-001, VAC-002 and VAC-008) vaccine, while one subject (VAC-010) received the
61 mRNA-1273 vaccine. Blood collection occurred at an average of 58 days post third vaccination dose. Subject
62 details are summarized in **Extended Data Table 1**. The frequency of CD19⁺CD27⁺IgD⁻IgM⁻ memory B cell

63 (MBCs) specific for the S protein⁺ was 6.18-fold higher in SN3 compared to SN2 (**Fig. 1a-b**). This was also 2.26-
64 fold higher than that previously observed in subjects with SARS-CoV-2 infection and subsequent vaccination
65 with two doses of the BNT162b2 mRNA vaccine (SP2)³. No major differences between the two groups were
66 observed in the CD19⁺CD27⁺IgD⁻IgM⁻/IgM⁺ memory B cell (MBCs) compartments (**Extended Data Fig. 1a-d**).
67 In addition, SN3 showed higher binding to the S protein, receptor binding domain (RBD) and N-terminal
68 domain (NTD), and a 5.82-fold higher neutralization activity against the original Wuhan SARS-CoV-2 virus
69 compared to SN2 (**Fig. 1c-d; Extended Data Fig. 1e-h**).

70

71 **Boosting antibody potency and breadth**

72 To evaluate the longitudinal B cell response, antigen specific class-switched MBCs (CD19⁺CD27⁺IgD⁻IgM⁻)
73 were single cell sorted using as bait the Wuhan prefusion SARS-CoV-2 S protein trimeric antigen which was
74 encoded by the mRNA vaccine. Sorted cells were incubated for two weeks to naturally release human
75 monoclonal antibodies (mAbs) into the supernatant. A total of 4,100 S protein⁺ MBCs were sorted and 2,436
76 (59.4%) produced mAbs able to recognize the S protein prefusion trimer in ELISA. Of these, 350 neutralized
77 the original Wuhan live SARS-CoV-2 virus when tested at a single point dilution (1:10) by cytopathic effect-
78 based microneutralization assay (CPE-MN). Overall, the fraction of S protein-specific B cells producing
79 neutralizing antibodies (nAbs) was 14.4% which is 2.2-fold higher than what observed in SN2 and comparable
80 to what observed for SP2 dose vaccinees (14.8%) in our previous study (**Extended Data Fig. 2a-b; Extended**
81 **Data Table 2**)³. To better characterize identified nAbs, we tried to express all 350 as immunoglobulin G1
82 (IgG1), and we were able to recover and express 206 of them. Binding by ELISA to RBD and NTD of the original
83 Wuhan SARS-CoV-2 S had similar frequency in SN2 and SN3, while we observed a reduction of S protein
84 trimer specific antibodies after a third booster dose, a trend similar to what observed in SP2 (**Extended Data**
85 **Fig. 2c**). No S2 domain binding nAbs were identified. Finally, we evaluated the neutralization potency against
86 the original Wuhan virus, the alpha (B.1.1.7), beta (B.1.351), gamma (P.1) delta (1.617.2), omicron BA.1
87 (B.1.1.529.1) and omicron BA.2 (B.1.1.529.2) and compared it with SN2 (**Fig. 1e-l**). To increase the power of
88 the analyses, in Fig.1 we included all 52 nAbs isolated from the five seronegative donors enrolled in our

89 previous study³. Overall, nAbs isolated in SN3 were higher in frequency and potency against all tested viruses
90 compared to SN2 and showed a significantly higher 100% inhibitory concentration (IC₁₀₀), except for BA.1 and
91 BA.2 VoCs, where SN2 did not have enough nAbs to make a meaningful comparison (**Fig. 1e-l**). The IC₁₀₀
92 geometric mean (GM-IC₁₀₀) in SN3 was 3.25, 7.57-, 3.31-, 3.21-, 5.70- and 2.83-fold lower compared to SN2
93 for the Wuhan virus, the alpha, beta, gamma, delta and BA.1 VoCs respectively (**Fig. 1; Extended Data Fig.**
94 **3**). Only for BA.2 a higher GM-IC₁₀₀ was observed in SN2 compared to SN3. Interestingly, SN3 also showed a
95 higher neutralization potency compared to SP2 against all tested viruses with a 1.13-, 3.49-, 2.81, 2.23-, 3.15-
96 , 2.22-, and 1.20-fold lower GM-IC₁₀₀ (**Fig. 1l; Extended Data Fig. 3**). In addition, we observed that nAbs
97 induced following a third booster dose retained a high ability to cross-neutralize all tested SARS-CoV-2 VoCs.
98 Indeed, while 67.3, 21.1, 25.0, 51.9, 1.9 and 7.7% of nAbs maintained the ability to neutralize alpha, beta,
99 gamma, delta, omicron BA.1 and omicron BA.2 respectively in the SN2 group³, the same viruses were
100 neutralized by 77.2, 41.7, 39.3, 61.2, 21.8 and 25.2% of nAbs in the SN3 group (**Fig. 1; Extended Data Table**
101 **2**). Finally, we assessed if a third booster dose would enhance the ability of nAbs to recognize and cross-
102 neutralize the distantly related SARS-CoV-1 virus. Two of the four SN3 donors presented nAbs able to
103 recognize SARS-CoV-1 (**Extended Data Fig. 4a**). However, only 2.4% (5/206) and 0.9% (2/206) of all nAbs were
104 able to bind the SARS-CoV-1 S protein and neutralize this sarbecovirus respectively, showing a lower
105 frequency than the one observed in SN2 and SP2 nAbs (**Extended Data Fig. 4a-b**)³.

106

107 **Antibody classes of cross-protection**

108 To understand the epitope region recognized by our RBD targeting-antibodies (*n* = 154) after a third
109 vaccination dose, we performed a competition assay with three known antibodies. As previously described,
110 we used the Class 1/2 antibody J08⁶, the Class 3 antibody S309⁷, and the Class 4 antibody CR3022⁸ to map
111 the epitope regions targeted by our RBD-binding nAbs³. The most abundant class of nAbs targeted the Class
112 1/2 epitope region (98/154; 63.6%), followed by Class 3 targeting nAbs (30/154; 19.5%) and nAbs that
113 recognize the Class 4 region (3/154; 1.9%). The remaining 23 (14.9%) nAbs did not compete with any of the
114 three antibodies used in our competition assay. As shown in **Fig. 2a**, in SN3 we observed a marked increase

115 in Class 3 and 4 nAbs compared to SN2 and a similar distribution to SP2. When we compared the GM-IC₁₀₀ of
116 classes of nAbs in the SN3 with the SN2 and SP2 groups, we observed similar neutralization potency when
117 tested against the SARS-CoV-2 virus originally isolated in Wuhan, China (**Extended Data Fig. 5**). Following, we
118 aimed to understand which classes of RBD ($n = 154$) and NTD ($n = 43$) targeting nAbs in SN3 were mainly
119 responsible for the cross-protection against the SARS-CoV-2 VoCs. Overall, we observed that Class 1/2 nAbs
120 are the most abundant family of antibodies against all tested variants, followed by Class 3, Not-competing,
121 NTD and Class 4 nAbs (**Fig. 2b-c**). Finally, we compared the functional antibody response between SN3 and
122 SP2 against the highly mutated omicron BA.1 and BA.2 viruses. Interestingly, we observed that a third mRNA
123 booster dose increases neutralization potency and evasion resistance of Class 1/2 nAbs against both omicron
124 BA.1 and BA.2 compared to SP2. The opposite trend was observed for Class 3 nAbs, which had a lower
125 frequency of cross-protection in SN3 compared to SP2 (**Fig. 2d-e**).
126

127 **Antibody gene repertoire**

128 We then interrogated the functional antibody repertoire. Initially, we analyzed all immunoglobulin heavy
129 chain sequences retrieved from the three different groups (SN2 $n = 58$; SN3 $n = 288$; SP2 $n = 278$), and their
130 respective V-J gene rearrangements (IGHV;IGHJ)³. Interestingly, SN2 and SN3 share only 20.2% percent
131 (23/114) of SN3 IGHV;IGHJ rearrangements, while SN3 and SP2 share up to 45.6% (52/114). In addition, we
132 observed that the frequency of antibodies encoded by predominant rearrangements induced by 2
133 vaccination doses (i.e. IGHV3-30;IGHJ6-1, IGHV3-33;IGHJ4-1, IGHV3-53;IGHJ6-1 and IGHV3-66;IGHJ4-1)^{3,6,9,10}
134 were reduced after a third booster dose, while we observed an expansion of the antibody germlines IGHV1-
135 58;IGHJ3-1 and IGHV1-69;IGHJ4-1 which were previously found to be predominant in SP2^{3,11} (**Fig. 3a**;
136 **Extended Data Fig. 6**). These latter germlines previously showed high level of cross-neutralization activity
137 against SARS-CoV-2 VoCs¹²⁻¹⁴. In addition, we observed in one donor (VAC-001) an important expansion of
138 the germline IGHV1-46;IGHJ6-1 after receiving a 3rd booster dose (**Fig. 3a; Extended Data Fig. 6**). Conversely
139 to what found in SP2³, we did not observe the expansion of the Class 3 targeting antibody germline IGHV2-
140 5;IGHJ4-1, which so far has been observed only in previously infected vaccinees or subjects immunized with

141 adenoviral vectors^{3,15,16}. Following, we aimed to identify expanded clonal families within the same four
142 donors after a second and third vaccination dose. Sequences (SN2 $n = 43$; SN3 $n = 288$) were clustered by
143 binning the clones to their inferred germlines (centroids) and according to 80% nucleotide sequence in the
144 heavy complementary determining region 3 (CDRH3). Clusters were defined as antibody families including at
145 least five or more members as previously described¹⁷. Of the 331 sequences, 226 (68.3%) were orphans (i.e.
146 did not cluster with other sequences), and only in six cases sequences from SN2 and SN3 were binned to the
147 same centroid (**Fig. 3b**). Only five clusters were identified, three of which were composed by antibodies
148 belonging exclusively from the SN3 group. Of these clusters, two were formed by antibody sequences shared
149 between the SN2 and SN3 groups. The smallest cluster was composed by 11 antibody members encoded
150 from the IGHV1-58;IGHJ3-1 germline, while the biggest cluster, composed by 18 antibody members, were
151 encoded by the IGHV3-48/IGHV3-53/IGHV3-66 germlines (**Fig. 3b**). Finally, we evaluated the V-gene mutation
152 levels, neutralization potency and breadth in nAbs encoded by reduced and expanded germlines following a
153 third vaccination dose. Our data showed that IGHV3-53;IGHJ6-1 and IGHV3-66;IGHJ4-1 germlines, expanded
154 in SN2 and reduced in SN3, have a similar level of V gene somatic mutations, are poorly cross-reactive
155 especially against omicron BA.1 and BA.2, and show medium neutralization potency (IC_{100} mainly between
156 100 and 1,000 ng ml⁻¹). Differently, the antibody germlines IGHV1-58;IGHJ3-1 and IGHV1-69;IGHJ4-1, mainly
157 expanded in SN3 and poorly represented in SN2, show between 5 and 15-fold higher V gene somatic
158 mutation levels, higher neutralization potency and breadth against all SARS-CoV-2 VoCs (**Fig. 3c-f**).
159

160 DISCUSSION

161 In agreement with other longitudinal studies^{9,10,18}, we found that a third dose of mRNA vaccine induces an
162 immune response similar to the hybrid immunity observed in people vaccinated after SARS-CoV-2 infection.
163 This antibody response is characterized by a small increase in S protein binding antibodies, a strong increase
164 in neutralizing potency and a considerable increase in antibodies able to cross-neutralize emerging variants,
165 including omicron BA.1 and BA.2. The increased potency and breadth are due to a significant expansion of S
166 protein specific MBCs, which is even higher than that observed in subjects with hybrid immunity, and by a

167 strong increase of V gene somatic mutations. What is new in our study is that the increased potency and
168 breadth observed after a third booster dose was due mostly to Class 1/2 nAbs, while Class 3 antibodies had
169 a lower frequency and breadth compared to subjects with hybrid immunity. In addition, we found that a third
170 mRNA dose did not induce a strong response against the distantly related SARS-CoV-1, suggesting that
171 additional doses of homologous vaccines against SARS-CoV-2 will focus the antibody response against this
172 virus instead of broadening cross-protection to other coronaviruses. Another unique observation of this
173 study is that the increased neutralization potency and breadth is not due to a linear evolution of the B cells
174 producing nAbs after two vaccine doses but is due mostly to the expansion of new B cells which were not
175 detected after primary immunization. Indeed, the secondary response induced by a third vaccine dose did
176 not derive from expanded B cell clones, but it was dominated by singlets that constituted 68% of the entire
177 repertoire. In addition, the germlines IGHV3-53;IGHJ6-1/IGHV3-66;IGHJ4-1 which dominated the neutralizing
178 response in donors infected with the original Wuhan virus and in subjects immunized with two doses of
179 mRNA vaccines^{3,6,19-21}, decreased in frequency and did not improve in potency or cross-neutralization after a
180 third dose. Conversely, the antibody germlines IGHV1-58;IGHJ3-1 and IGHV1-69;IGHJ4-1 became largely
181 responsible for the improved potency and cross-neutralization observed after a third dose. Interestingly, the
182 IGHV1-58 germline predominant in this group was previously shown to recognize a “supersite” on the S
183 protein surface and to be expanded following beta or omicron breakthrough infection in vaccinated
184 individuals^{12,14,22}. A unique observation of this work is that the highly cross-reactive germline IGHV2-5;IGHJ4-
185 1, found in subjects with hybrid immunity and in people vaccinated with viral vectors^{3,16}, is absent after a
186 third mRNA vaccine, suggesting that the induction of this germline may require endogenous production of
187 the S protein. The lack of expansion of the IGHV2-5;IGHJ4-1 germline after three mRNA vaccine doses could
188 partially explain the above mentioned loss of cross-reactivity by Class 3 nAbs. Overall, our study provides a
189 high-resolution picture of the functional and genetic properties of a third mRNA vaccination and, despite we
190 observed important similarities with the hybrid immunity, unravels features of the antibody response
191 uniquely produced after a third mRNA vaccine dose. These observations are very important and should be
192 considered while designing new vaccines and implementing vaccination regimens for booster doses,

193 especially in low-middle income countries where less than 20% of people received at least one dose of
194 vaccines²³.

195 REFERENCES

196 1. Hoffmann, M., *et al.* The Omicron variant is highly resistant against antibody-mediated
197 neutralization: Implications for control of the COVID-19 pandemic. *Cell* **185**, 447-456.e411 (2022).

198 2. Karim, S.S.A. & Karim, Q.A. Omicron SARS-CoV-2 variant: a new chapter in the COVID-19 pandemic.
199 *Lancet (London, England)* **398**, 2126-2128 (2021).

200 3. Andreano, E., *et al.* Hybrid immunity improves B cells and antibodies against SARS-CoV-2 variants.
201 *Nature* **600**, 530-535 (2021).

202 4. Tregoning, J.S., Flight, K.E., Higham, S.L., Wang, Z. & Pierce, B.F. Progress of the COVID-19 vaccine
203 effort: viruses, vaccines and variants versus efficacy, effectiveness and escape. *Nature Reviews
204 Immunology* **21**, 626-636 (2021).

205 5. Andreano, E. & Rappuoli, R. SARS-CoV-2 escaped natural immunity, raising questions about vaccines
206 and therapies. *Nature Medicine* **27**, 759-761 (2021).

207 6. Andreano, E., *et al.* Extremely potent human monoclonal antibodies from COVID-19 convalescent
208 patients. *Cell* **184**, 1821-1835.e1816 (2021).

209 7. Pinto, D., *et al.* Cross-neutralization of SARS-CoV-2 by a human monoclonal SARS-CoV antibody.
210 *Nature* **583**, 290-295 (2020).

211 8. Yuan, M., *et al.* A highly conserved cryptic epitope in the receptor binding domains of SARS-CoV-2
212 and SARS-CoV. *Science* **368**, 630-633 (2020).

213 9. Muecksch, F., *et al.* Increased Memory B Cell Potency and Breadth After a SARS-CoV-2 mRNA Boost.
214 *Nature* (2022).

215 10. Wang, Z., *et al.* Naturally enhanced neutralizing breadth against SARS-CoV-2 one year after infection.
216 *Nature* **595**, 426-431 (2021).

217 11. Andreano, E., *et al.* Anatomy of Omicron neutralizing antibodies in COVID-19 mRNA vaccinees.
218 *Research Square* (2022).

219 12. Wang, L., *et al.* Ultrapotent antibodies against diverse and highly transmissible SARS-CoV-2 variants.
220 *Science* **373**, eabh1766 (2021).

221 13. Zhou, T., *et al.* Structural basis for potent antibody neutralization of SARS-CoV-2 variants including
222 B.1.1.529. *Science* **376**, eabn8897 (2022).

223 14. Kaku, C.I., *et al.* Recall of pre-existing cross-reactive B cell memory following Omicron breakthrough
224 infection. *bioRxiv*, 2022.2004.2001.486726 (2022).

225 15. Lee, H.K., *et al.* mRNA vaccination in octogenarians 15 and 20 months after recovery from
226 COVID-19 elicits robust immune and antibody responses that include Omicron. *Cell Reports* **39**(2022).

227 16. Chi, X., *et al.* Broadly neutralizing antibodies against Omicron-included SARS-CoV-2 variants induced
228 by vaccination. *Signal Transduction and Targeted Therapy* **7**, 139 (2022).

229 17. Chen, E.C., *et al.* Systematic analysis of human antibody response to ebolavirus glycoprotein reveals
230 high prevalence of neutralizing public clonotypes. *bioRxiv*, 2022.2001.2012.476089 (2022).

231 18. Goel, R.R., *et al.* Efficient recall of Omicron-reactive B cell memory after a third dose of SARS-CoV-2
232 mRNA vaccine. *Cell* (2022).

233 19. Barnes, C.O., *et al.* Structures of Human Antibodies Bound to SARS-CoV-2 Spike Reveal Common
234 Epitopes and Recurrent Features of Antibodies. *Cell* **182**, 828-842.e816 (2020).

235 20. Zhang, Q., *et al.* Potent and protective IGHV3-53/3-66 public antibodies and their shared escape
236 mutant on the spike of SARS-CoV-2. *Nature Communications* **12**, 4210 (2021).

237 21. Andreano, E. & Rappuoli, R. Immunodominant antibody germlines in COVID-19. *The Journal of
238 experimental medicine* **218**(2021).

239 22. Reincke, S.M., *et al.* SARS-CoV-2 Beta variant infection elicits potent lineage-specific and cross-
240 reactive antibodies. **375**, 782-787 (2022).

241 23. Global Dashboard for Vaccine Equity. *United Nations Development Programme (UNDP) - Data
242 Futures Platform* (2022).

243 **FIGURE LEGENDS**

244 **Fig. 1. Potency and breadth of neutralization of nAbs against SARS-CoV-2 and VoCs. a,** The graph shows the
245 frequency of CD19⁺CD27⁺IgD⁺IgM⁻ able to bind the SARS-CoV-2 S protein trimer (S protein⁺) in SN2 and SN3
246 donors ($n = 4/\text{group}$). Black line and bars denote the geometric mean. **b,** The table summarizes the
247 frequencies of the B cell populations in SN2 and SN3. **c,** The graph shows the neutralizing activity of plasma
248 samples against the original Wuhan SARS-CoV-2 virus. Technical duplicates were performed for each
249 experiment. **d,** The table summarizes the 100% inhibitory dilution (ID_{100}) of each COVID-19 vaccinee and the
250 geometric mean for SN2 and SN3 ($n = 4/\text{group}$). **e-k,** Scatter dot charts show the neutralization potency,
251 reported as IC_{100} (ng ml^{-1}), of nAbs tested against the original Wuhan SARS-CoV-2 virus (**e**) and the alpha (**f**),
252 beta (**g**), gamma (**h**), delta (**i**), omicron BA.1 (**j**) and omicron BA.2 (**k**) VoCs. The number and percentage of
253 nAbs from SN2 vs SN3, fold-change and statistical significance are denoted on each graph. **l,** The table shows
254 the IC_{100} geometric mean (GM) of all nAbs pulled together from SN2, SN3 and SP2 against all SARS-CoV-2
255 viruses tested. “†” indicates previously published data³. Technical duplicates were performed for each
256 experiment. A nonparametric Mann–Whitney t test was used to evaluate statistical significances between
257 groups. Two-tailed p-value significances are shown as * $p < 0.05$, ** $p < 0.01$, *** $p < 0.001$, and **** $p <$
258 0.0001.

259

260 **Fig. 2. Distribution of SN3 nAbs against SARS-CoV-2 VoCs. a,** The bar graph shows the epitope regions
261 recognized by RBD-binding nAbs. Class 1/2, Class 3, Class 4 and Not-competing nAbs are shown in light blue,
262 orange, green and light gray respectively. The number (n) of antibodies tested per each donor is denoted on
263 the graph. Right panel highlights the epitope recognized by Class 1/2 (J08), Class 3 (S309) and Class 4 (CR3022)
264 antibodies used in our competition assay. **b,** Pie charts show the distribution of cross-protective nAbs based
265 on their ability to bind Class 1/2, Class 3 and Class 4 regions on the RBD, as well as not-competing nAbs (gray)
266 and NTD-targeting nAbs (cyan). Dot charts show the neutralization potency, reported as IC_{100} (ng ml^{-1}), of
267 nAbs against the Wuhan virus and alpha, beta, gamma, delta, omicron BA.1 and omicron BA.2 SRS-CoV-2
268 VoCs observed in the SN3 group. The number and percentage of nAbs are denoted on each graph. **c,** the

269 table summarizes number and percentages of Class 1/2, Class 3, Class 4, not-competing and NTD-targeting
270 nAbs for each tested variant. **d-e**, dot charts compare the distribution of nAbs between SN3 and SP2 groups
271 against omicron BA.1 (**d**) and BA.2 (**e**). The number, percentage and GM-IC₁₀₀ (black lines and colored bars)
272 of nAbs are denoted on each graphs.

273

274 **Fig. 3. Repertoire analyses and characterization of predominant antibody germlines. a**, Radar plot shows
275 the distribution of IGHV;IGHJ germlines among the three different groups. SN2, SN3 and SP2 are shown in
276 light blue, dark blue and red respectively. Heatmap represents the Log2 fold change (FC) among groups. **b**,
277 Network plot shows the clonally-expanded antibody families in SN2 and SN3. Centroids, nAbs from SN2 and
278 SN3 groups are shown in gray, light blue and dark blue respectively. Clusters and expanded clones are
279 highlighted in bright green and bright purple respectively. **c-f**, The graphs show the V gene somatic mutation
280 frequency (left panel) and neutralization potency (IC₁₀₀; right panel) of IGHV3-53;IGHJ6-1 (**c**), IGHV3-
281 66;IGHJ4-1 (**d**), IGHV1-58;IGHJ3-1 (**e**), and IGHV1-69;IGHJ4-1 (**f**) gene derived nAbs, against the original SARS-
282 CoV-2 virus first detected in Wuhan, China, and all SARS-CoV-2 VoCs. The number and percentage of nAbs
283 analyzed are denoted on each graph.

284 **METHODS**

285 **Enrollment of COVID-19 vaccinees and human sample collection**

286 This work results from a collaboration with the Azienda Ospedaliera Universitaria Senese, Siena (IT) that
287 provided samples from COVID-19 vaccinated donors, of both sexes, who gave their written consent. The
288 study was approved by the Comitato Etico di Area Vasta Sud Est (CEAVSE) ethics committees (Parere 17065
289 in Siena) and conducted according to good clinical practice in accordance with the declaration of Helsinki
290 (European Council 2001, US Code of Federal Regulations, ICH 1997). This study was unblinded and not
291 randomized. No statistical methods were used to predetermine sample size.

292

293 **Single cell sorting of SARS-CoV-2 S protein⁺ memory B cells from COVID-19 vaccinees**

294 Peripheral blood mononuclear cells (PBMCs) and single cell sorting strategy were performed as previously
295 described^{3,6}. Briefly, PBMC were isolated from heparin-treated whole blood by density gradient
296 centrifugation (Ficoll-PaqueTM PREMIUM, Sigma-Aldrich) and stained with Live/Dead Fixable Aqua
297 (Invitrogen; Thermo Scientific) diluted 1:500. After 20 min incubation cells were saturated with 20% normal
298 rabbit serum (Life technologies) for 20 min at 4°C and then stained with SARS-CoV-2 S-protein labeled with
299 Strep-Tactin[®]XT DY-488 (iba-lifesciences cat# 2-1562-050) for 30 min at 4°C. After incubation the following
300 staining mix was used CD19 V421 (BD cat# 562440, 1:320), IgM PerCP-Cy5.5 (BD cat# 561285, 1:50), CD27 PE
301 (BD cat# 340425, 1:30), IgD-A700 (BD cat# 561302, 1:15), CD3 PE-Cy7 (BioLegend cat# 300420, 1:100), CD14
302 PE-Cy7 (BioLegend cat# 301814, 1:320), CD56 PE-Cy7 (BioLegend cat# 318318, 1:80) and cells were incubated
303 at 4°C for additional 30 min. Stained MBCs were single cell-sorted with a BD FACS Aria III (BD Biosciences)
304 into 384-well plates containing 3T3-CD40L feeder cells, IL-2 and IL-21 and incubated for 14 days as previously
305 described²⁴.

306

307 **ELISA assay with SARS-CoV-2 and SARS-CoV-1 S protein prefusion trimer**

308 mAbs and plasma binding specificity against the S-protein trimer was detected by ELISA as previously
309 described³. Briefly, 384-well plates (microplate clear, Greiner Bio-one) were coated with 3 µg/mL of

310 streptavidin (Thermo Fisher) diluted in carbonate-bicarbonate buffer (E107, Bethyl laboratories) and
311 incubated at RT overnight. The next day, plates were incubated 1 h at RT with 3 µg/mL of SARS-CoV-2 or
312 SARS-CoV-1 S protein, and saturated with 50 µL/well of blocking buffer (phosphate-buffered saline, 1% BSA)
313 for 1 h at 37°C. Following, 25 µL/well of mAbs or plasma samples, diluted 1:5 or 1:10 respectively in sample
314 buffer (phosphate-buffered saline, 1% BSA, 0.05% Tween-20), were added serially diluted step dilution 1:2
315 and then incubated at 1 h at 37°C. Finally, 25 µL/well of alkaline phosphatase-conjugated goat antihuman
316 IgG and IgA (Southern Biotech) diluted 1:2000 in sample buffer were added. S protein binding was detected
317 using 25 µL/well of PNPP (p-nitrophenyl phosphate; Thermo Fisher) and the reaction was measured at a
318 wavelength of 405 nm by the Varioskan Lux Reader (Thermo Fisher Scientific). After each incubation step,
319 plates were washed three times with 100 µL/well of washing buffer (phosphate-buffered saline, 0.05%
320 Tween-20). Sample buffer was used as a blank and the threshold for sample positivity was set at 2-fold the
321 optical density (OD) of the blank. Technical duplicates were performed for mAbs and technical triplicates
322 were performed for sera samples.

323

324 **ELISA assay with RBD, NTD and S2 subunits**

325 mAbs identification and plasma screening of vaccinees against RBD, NTD or S2 SARS-CoV-2 protein were
326 performed by ELISA as previously described³. Briefly, 3 µg/mL of RBD, NTD or S2 SARS-CoV-2 protein diluted
327 in carbonate-bicarbonate buffer (E107, Bethyl laboratories) were coated in 384-well plates (microplate clear,
328 Greiner Bio-one) and blocked with 50 µL/well of blocking buffer (phosphate-buffered saline, 1% BSA) for 1h
329 at 37°C. After washing, plates were incubated 1 h at 37 °C with mAbs diluted 1:5 in samples buffer
330 (phosphate-buffered saline, 1% BSA, 0.05% Tween-20) or with plasma at a starting dilution 1:10 and step
331 diluted 1:2 in sample buffer. Anti-Human IgG –Peroxidase antibody (Fab specific) produced in goat (Sigma)
332 diluted 1:45000 in sample buffer was then added and samples incubated for 1 h at 37°C. Plates were then
333 washed, incubated with TMB substrate (Sigma) for 15 min before adding the stop solution (H₂SO₄ 0.2M). The
334 OD values were identified using the Varioskan Lux Reader (Thermo Fisher Scientific) at 450 nm. Each

335 condition was tested in triplicate and samples tested were considered positive if OD value was 2-fold the
336 blank.

337

338 **Flow cytometry-based competition assay**

339 To classify mAbs candidates on the basis of their interaction with Spike epitopes, we performed a flow
340 cytometry-based competition assay as previously described^{3,11}. Briefly, magnetic beads (Dynabeads His-Tag,
341 Invitrogen) were coated with histidine tagged S protein according to the manufacturers' instructions. Then,
342 20 µg/mL of coated S protein-beads were pre-incubated with unlabeled nAbs diluted 1:2 in PBS for 40
343 minutes at RT. After incubation, the mix Beads-antibody was washed with 100 µL of PBS-BSA 1%. Then, to
344 analyze epitope competition, mAbs able to bind RBD Class 1/2, (J08), Class 3 (S309) and Class 4 (CR3022)
345 were labeled with three different fluorophores (Alexa Fluor 647, 488 and 594) using Alexa Fluor NHS Ester
346 kit (Thermo Scientific), were mixed and incubated with S-protein-beads. Following 40 minutes of incubation
347 at RT, the mix Beads-antibodies was washed with PBS, resuspended in 150 µL of PBS-BSA 1% and analyzed
348 using BD LSR II flow cytometer (Becton Dickinson). Beads with or without S-protein incubated with labeled
349 antibodies mix were used as positive and negative control respectively. FACSDiva Software (version 9) was
350 used for data acquisition and analysis was performed using FlowJo (version 10).

351

352 **SARS-CoV-2 authentic viruses neutralization assay**

353 All SARS-CoV-2 authentic virus neutralization assays were performed in the biosafety level 3 (BSL3)
354 laboratories at Toscana Life Sciences in Siena (Italy) and Vismederi Srl, Siena (Italy). BSL3 laboratories are
355 approved by a Certified Biosafety Professional and are inspected every year by local authorities. To evaluate
356 the neutralization activity of identified nAbs against SARS-CoV-2 and all VoCs and evaluate the breadth of
357 neutralization of this antibody is a cytopathic effect-based microneutralization assay (CPE-MN) was
358 performed^{3,6}. Briefly, the CPE-based neutralization assay sees the co-incubation of the antibody with a SARS-
359 CoV-2 viral solution containing 100 median Tissue Culture Infectious Dose (100 TCID₅₀) of virus for 1 hour at
360 37°C, 5% CO₂. The mixture was then added to the wells of a 96-well plate containing a sub-confluent Vero E6

361 cell monolayer. Plates were incubated for 3-4 days at 37°C in a humidified environment with 5% CO₂, then
362 examined for CPE by means of an inverted optical microscope by two independent operators. All nAbs were
363 tested a starting dilution of 1:5 and the IC₁₀₀ evaluated based on their initial concentration while plasma
364 samples were tested starting from a 1:10 dilution. Both nAbs and plasma samples were then diluted step 1:2.
365 Technical duplicates were performed for both nAbs and plasma samples. In each plate positive and negative
366 control were used as previously described⁵.

367

368 **SARS-CoV-2 virus variants CPE-MN neutralization assay**

369 The SARS-CoV-2 viruses used to perform the CPE-MN neutralization assay were the original Wuhan SARS-
370 CoV-2 virus (SARS-CoV-2/INMI1-Isolate/2020/Italy: MT066156), SARS-CoV-2 B.1.1.7 (INMI GISAID accession
371 number: EPI_ISL_736997), SARS-CoV-2 B.1.351 (EVAg Cod: 014V-04058), B.1.1.248 (EVAg CoD: 014V-04089)
372 and B.1.617.2 (GISAID ID: EPI_ISL_2029113)²⁶.

373

374 **HEK293TN- hACE2 cell line generation**

375 HEK293TN- hACE2 cell line was generated by lentiviral transduction of HEK293TN (System Bioscience) cells
376 as described in Notarbartolo S. et al²⁵. Lentiviral vectors were produced following a standard procedure based
377 on calcium phosphate co-transfection with 3rd generation helper and transfer plasmids. The transfer vector
378 pLENTI_hACE2_HygR was obtained by cloning of hACE2 from pcDNA3.1-hACE2 (Addgene #145033) into
379 pLenti-CMV-GFP-Hygro (Addgene #17446). HEK293TN-hACE2 cells were maintained in DMEM,
380 supplemented with 10% FBS, 1% glutamine, 1% penicillin/streptomycin and 250 µg/ml Hygromycin (GIBCO).

381

382 **Production of SARS-CoV-1 pseudoparticles**

383 SARS-CoV-1 lentiviral pseudotype particles were generated as described in Conforti et al. for SARS-CoV-2²⁶
384 by using the SARS-CoV1 SPIKE plasmid pcDNA3.3_CoV1_D28 (Addgene plasmid # 170447).

385

386 **SARS-CoV-1 neutralization assay**

387 For neutralization assay, HEK293TN-hACE2 cells were plated in white 96-well plates in complete DMEM
388 medium. 24h later, cells were infected with 0.1 MOI of SARS-CoV-1 pseudoparticles that were previously
389 incubated with serial dilution of purified or not purified (cell supernatant) mAb. In particular, a 7-point dose-
390 response curve (plus PBS as untreated control), was obtained by diluting mAb or supernatant respectively
391 five-fold and three-fold. Thereafter, nAbs of each dose-response curve point was added to the medium
392 containing SARS-CoV-1 pseudoparticles adjusted to contain 0.1 MOI. After incubation for 1h at 37°C, 50 µl of
393 mAb/SARS-CoV-1 pseudoparticles mixture was added to each well and plates were incubated for 24h at 37°C.
394 Each point was assayed in technical triplicates. After 24h of incubation cell infection was measured by
395 luciferase assay using Bright-Glo™ Luciferase System (Promega) and Infinite F200 plate reader (Tecan) was
396 used to read luminescence. Obtained relative light units (RLUs) were normalized to controls and dose
397 response curve were generated by nonlinear regression curve fitting with GraphPad Prism to calculate
398 Neutralization Dose 50 (ND₅₀).

399

400 **Single cell RT-PCR and Ig gene amplification and transcriptionally active PCR expression**

401 To express our nAbs as full-length IgG1, 5 µL of cell lysate from the original 384-cell sorting plate were used
402 for reverse transcription polymerase chain reaction (RT-PCR), and two rounds of PCRs (PCRI and PCRII-
403 nested) as previously described^{3,6}. Obtained PCRII products will be used to recover the antibody heavy and
404 light chain sequences, through Sanger sequencing, and for antibody cloning into expression vectors as
405 previously described^{27,28}. Transcriptionally active PCR (TAP) reaction was performed using 5 µL of Q5
406 polymerase (NEB), 5 µL of GC Enhancer (NEB), 5 µL of 5X buffer, 10 mM dNTPs, 0.125 µL of forward/reverse
407 primers and 3 µL of ligation product, using the following cycles: 98°/2', 35 cycles 98°/10'', 61°/20'', 72°/1'
408 and 72°/5'. TAP products were purified under the same PCRII conditions, quantified by Qubit Fluorometric
409 Quantitation assay (Invitrogen) and used for transient transfection in Expi293F cell line following
410 manufacturing instructions.

411

412 **Functional repertoire analyses**

413 nAbs VH and VL sequence reads were manually curated and retrieved using CLC sequence viewer (Qiagen).
414 Aberrant sequences were removed from the data set. Analyzed reads were saved in FASTA format and the
415 repertoire analyses was performed using Cloanalyst
416 (<http://www.bu.edu/computationalimmunology/research/software/>)^{29,30}.

417

418 **Radar plot distribution of IGHV;IGHJ germlines**

419 A radar plot was generated to display the distribution of IGHV;IGHJ germlines among the three nAbs groups:
420 seronegative 2nd dose, 3rd dose and seropositive 2nd dose. Each star in the radar represents a particular
421 IGHV;IGHJ germline combination, alphabetically sorted. Germline abundance is represented as percentage
422 of the total of each group. In addition, the log2 fold change for each combination of the three groups was
423 calculated and represented as a concentric heatmap; the higher the fold change it is, the bigger is the first
424 group with respect to the other, and vice versa. The figure was generated with R v4.1.1. and assembled with
425 ggplot2 v3.3.5.

426

427 **Network plot of clonally expanded antibody families**

428 To investigate the genetic similarity within and between lineages, a network map was built by representing
429 each clonal family with a centroid and connecting centroids sharing a similar sequence. The centroid
430 sequence was computed with Cloanalyst to represent the average CDRH3 sequence for each clonal family,
431 and Hamming distance was calculated for each antibody CDRH3 sequence to represent the relationship
432 within the clonal family. Levenshtein distance was calculated between each centroid representative of each
433 clonal family to investigate the relationship between clonal families. Levenshtein distance was calculated
434 with the R package stringdistm v0.9.8 (<https://cran.r-project.org/web/packages/stringdist/index.html>) and
435 normalized between 0 and 1. A network graph was generated with the R package ggraph v2.0.5
436 (<https://ggraph.data-imaginist.com/index.html>) with Fruchterman-Reingold layout algorithm and the figure
437 was assembled with ggplot2 v3.3.5. The size of the centroid is proportional to the number of antibodies

438 belonging to the same clonal family, while the color of each node represents the antibody origin: light blue
439 and dark blue for seronegative 2nd dose and seronegative 3rd dose, respectively.

440

441 **Statistical analysis**

442 Statistical analysis was assessed with GraphPad Prism Version 8.0.2 (GraphPad Software, Inc., San Diego, CA).
443 Nonparametric Mann-Whitney t test was used to evaluate statistical significance between the two groups
444 analyzed in this study. Statistical significance was shown as * for values ≤ 0.05 , ** for values ≤ 0.01 , *** for
445 values ≤ 0.001 , and **** for values ≤ 0.0001 .

446 **METHODS REFERENCES**

447 24. Huang, J., *et al.* Isolation of human monoclonal antibodies from peripheral blood B cells. *Nature Protocols* **8**, 1907-1915 (2013).

448 25. Notarbartolo, S., *et al.* Integrated longitudinal immunophenotypic, transcriptional and repertoire analyses delineate immune responses in COVID-19 patients. *Science immunology* **6**(2021).

449 26. Conforti, A., *et al.* COVID-eVax, an electroporated DNA vaccine candidate encoding the SARS-CoV-2 RBD, elicits protective responses in animal models. *Molecular Therapy* **30**, 311-326 (2022).

450 27. Wardemann, H. & Busse, C.E. Expression Cloning of Antibodies from Single Human B Cells. *Methods in molecular biology (Clifton, N.J.)* **1956**, 105-125 (2019).

451 28. Tiller, T., *et al.* Efficient generation of monoclonal antibodies from single human B cells by single cell RT-PCR and expression vector cloning. *Journal of immunological methods* **329**, 112-124 (2008).

452 29. Kepler, T.B. Reconstructing a B-cell clonal lineage. I. Statistical inference of unobserved ancestors. *F1000Res* **2**, 103-103 (2013).

453 30. Kepler, T.B., *et al.* Reconstructing a B-Cell Clonal Lineage. II. Mutation, Selection, and Affinity Maturation. *5*(2014).

454

455

456

457

458

459

460

461 **Acknowledgments**

462 This work was funded by the European Research Council (ERC) advanced grant agreement number 787552
463 (vAMRes). This work was supported by a fundraising activity promoted by Unicoop Firenze, Coop Alleanza
464 3.0, Unicoop Tirreno, Coop Centro Italia, Coop Reno e Coop Amiatina. This publication was supported by the
465 COVID-2020-12371817 project, which received funding from the Italian Ministry of Health. We would also
466 like to acknowledge Dr. Jason McLellan, for kindly providing the S protein trimer, RBD, NTD and S2 constructs,
467 Dr. Olivier Schwartz, for providing the B.1.617.2 (delta) SARS-CoV-2 variant, and Dr. Piet Maes for providing
468 the B.1.1.529.1 (BA.1) and B.1.1.529.2 (BA.2) SARS-CoV-2 variants. We would like to thank the nurse staff of
469 the operative unit of the department of Medical Sciences, Infectious and Tropical Diseases Unit, Siena
470 University Hospital, Siena, Italy, and all the COVID-19 vaccinated donors for participating to this study.

471

472 **Author contributions**

473 Conceived the study: E.A. and R.R.; Enrolled COVID-19 vaccinees: F.M., M.F., I.R. and M.T.; Performed PBMC
474 isolation and single cell sorting: E.A and I.P.; Performed ELISAs and competition assays: I.P., V.A., G.A.;
475 Recovered nAbs VH and VL and expressed antibodies: I.P. and N.M.; Recovered VH and VL sequences and
476 performed the repertoire analyses: P.P., E.A. and G.M.; Produced and purified SARS-CoV-2 S protein
477 constructs: E.P.; Performed neutralization assays in BSL3 facilities: E.A., G. Pie., G.Pic., M.L., L.B. and G.G.;
478 Performed SARS-CoV-1 pseudotype neutralization assays: S.M. and L.D.; Supported day-by-day laboratory
479 activities and management: C.D.S.; Manuscript writing: E.A. and R.R.; Final revision of the manuscript: E.A.,
480 I.P., G.Pie., G.Pic., V.A., G.A., P.P., N.M., E.P., L.B., G.G., M.L., S.M., L.D., C.D.S., M.F., I.R., M.T., F.M., C.S.,
481 R.D.F., E.M. and R.R.; Coordinated the project: E.A., C.S., E.M., R.D.F. and R.R.

482

483 **Competing interests**

484 R.R. is an employee of GSK group of companies. E.A., I.P., N.M., P.P., E.P., V.A., C.D.S., C.S. and R.R. are listed
485 as inventors of full-length human monoclonal antibodies described in Italian patent applications n.
486 102020000015754 filed on June 30th 2020, 102020000018955 filed on August 3rd 2020 and

487 102020000029969 filed on 4th of December 2020, and the international patent system number
488 PCT/IB2021/055755 filed on the 28th of June 2021. All patents were submitted by Fondazione Toscana Life
489 Sciences, Siena, Italy. R.D.F. is a consultant for Moderna on activities not related to SARS-CoV-2. Remaining
490 authors have no competing interests to declare.

491

492 **Additional information**

493 **Correspondence and requests for materials** should be addressed to R.R.

494

495 **Data availability**

496 Source data are provided with this paper. All data supporting the findings in this study are available within
497 the article or can be obtained from the corresponding author upon request.

498 **EXTENDED DATA FIGURES**

499 **Extended Data Fig. 1. B cell frequencies and polyclonal response.** **a-c**, The graph shows the frequency of
500 CD19⁺CD27⁺IgD⁻IgM⁻ (**a**) and IgM⁺ (**b**), and CD19⁺CD27⁺IgD⁻IgM⁺ able to bind the SARS-CoV-2 S protein trimer
501 (S protein⁺) (**c**) in SN2 and SN3 ($n = 4$ /group). Black line and bars denote the geometric mean. **d**, The table
502 summarizes the frequencies of the B cell populations for the SN3 group. **e-g**, Graphs show the ability of
503 plasma samples from SN2 and SN3 to bind the S protein trimer (**e**), RBD (**f**) and NTD (**g**). Mean and standard
504 deviation are denoted on each graph. Technical triplicates were performed for each experiment. **h**, The table
505 summarizes the binding titers of each COVID-19 vaccinee and the geometric mean for SN2 and SN3. A
506 nonparametric Mann–Whitney t test was used to evaluate statistical significances between groups. Two-
507 tailed p-value significances are shown as * $p < 0.05$, ** $p < 0.01$, *** $p < 0.001$, and **** $p < 0.0001$.

508

509 **Extended Data Fig. 2. Identification of SARS-CoV-2 S protein-specific nAbs.** **a**, The graph shows supernatants
510 tested for binding to the Wuhan SARS-CoV-2 S protein antigen. Threshold of positivity has been set as two
511 times the value of the blank (dotted line). Light blue, dark blue and red dots represent mAbs that bind to the
512 S protein for SN2 and SN3, and SP2 respectively. Light gray dots represent mAbs that did not bind the S
513 protein. **b**, The bar graph shows the percentage of not-neutralizing (gray), neutralizing mAbs from SN2 (light
514 blue), neutralizing mAbs for SN3 (dark blue) and neutralizing mAbs for SP2 (red). The total number (n) of
515 antibodies tested per individual is shown on top of each bar. **c**, The graph shows the percentage of nAbs that
516 bind specifically the RBD (dark gray), the NTD (cyan) or that did not bind single domains but recognized
517 exclusively the S protein in its trimetric conformation (light gray). The number (n) of tested nAbs per donor
518 is reported on top of each bar. Technical duplicates were performed for each experiment.

519

520 **Extended Data Fig. 3. Fold-change neutralization potency against SARS-CoV-2 VoCs.** **a-g**, The graphs show
521 the fold-change neutralization potency shown as GM-IC₁₀₀ (ng ml⁻¹) among SN2 (light blue), SN3 (dark blue)
522 and SP2 (red). Fold-changes are denoted on each graph.

523

524 **Extended Data Fig. 4. Functional characterization of SARS-CoV-1 nAbs.** **a**, The bar graph shows the
525 percentage of not-binding antibodies (grey), and SARS-CoV-1 binding nAbs for SN3 (dark blue), SN2 (light
526 blue) and SP2 (red). The total number (n) of antibodies tested per individual is shown on the top of each bar.
527 **b**, Dot chart shows the neutralization potency, reported as 50% neutralizing dilution (ND_{50} ng ml $^{-1}$), of nAbs
528 isolated from SN3 (dark blue), SN2 (light blue) and SP2 (red). The number and percentage of nAbs from
529 individuals who were seronegative and seropositive and neutralization ND_{50} (ng ml $^{-1}$) ranges (black dotted
530 lines) are denoted on the graph.

531

532 **Extended Data Fig. 5. Epitope mapping of RBD-targeting nAbs.** **a-c**, Dot charts show the distribution of Class
533 1/2 (**a**), Class 3 (**b**) and Class 4 (**c**) nAbs against the original SARS-CoV-2 virus first detected in Wuhan for nAbs
534 isolated from SN2, SN3 and SP2. The number and percentage of nAbs and neutralization IC_{100} geometric mean
535 (black lines, light blue, orange and green bars) are denoted on each graph. **d**, the table summarizes the IC_{100}
536 geometric mean of nAbs against Wuhan for all tested groups.

537

538 **Extended Data Fig. 6. Antibody germline distribution.** The graph shows the IGHV;IGHJ rearrangement
539 frequencies among SN2 (light blue), SN3 (dark blue) and SP2 (red) dose vaccinees (right panel), and the
540 frequency within SN3 subjects (left panel).

541 **EXTENDED DATA TABLES**

542 **Extended Data Table 1. Clinical details of COVID-19 vaccinees.**

543

544 **Extended Data Table 2. Summary of sorted B cells and neutralizing antibodies against SARS-CoV-2 and**

545 **VoCs.**

Figure 1

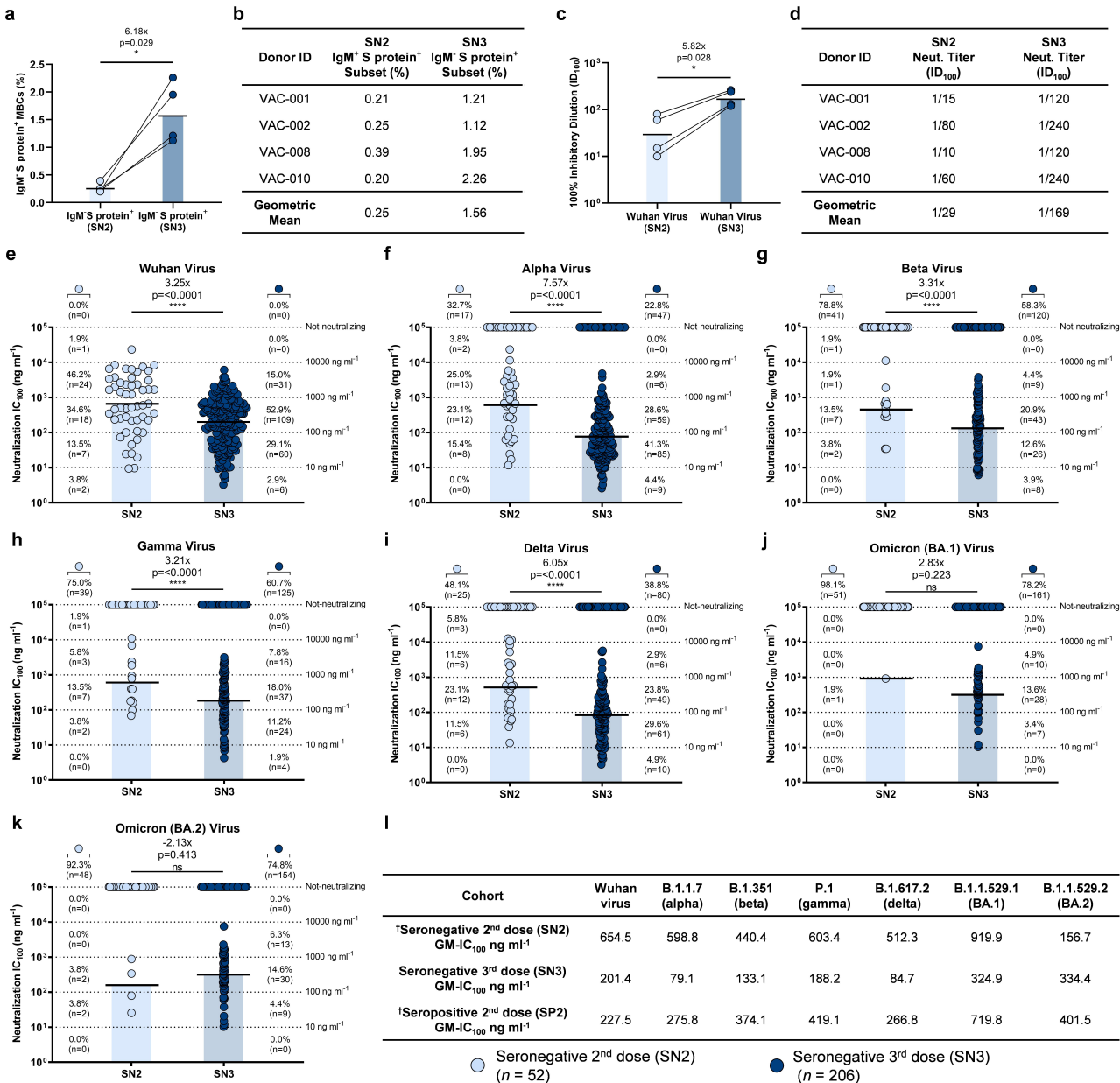


Figure 2

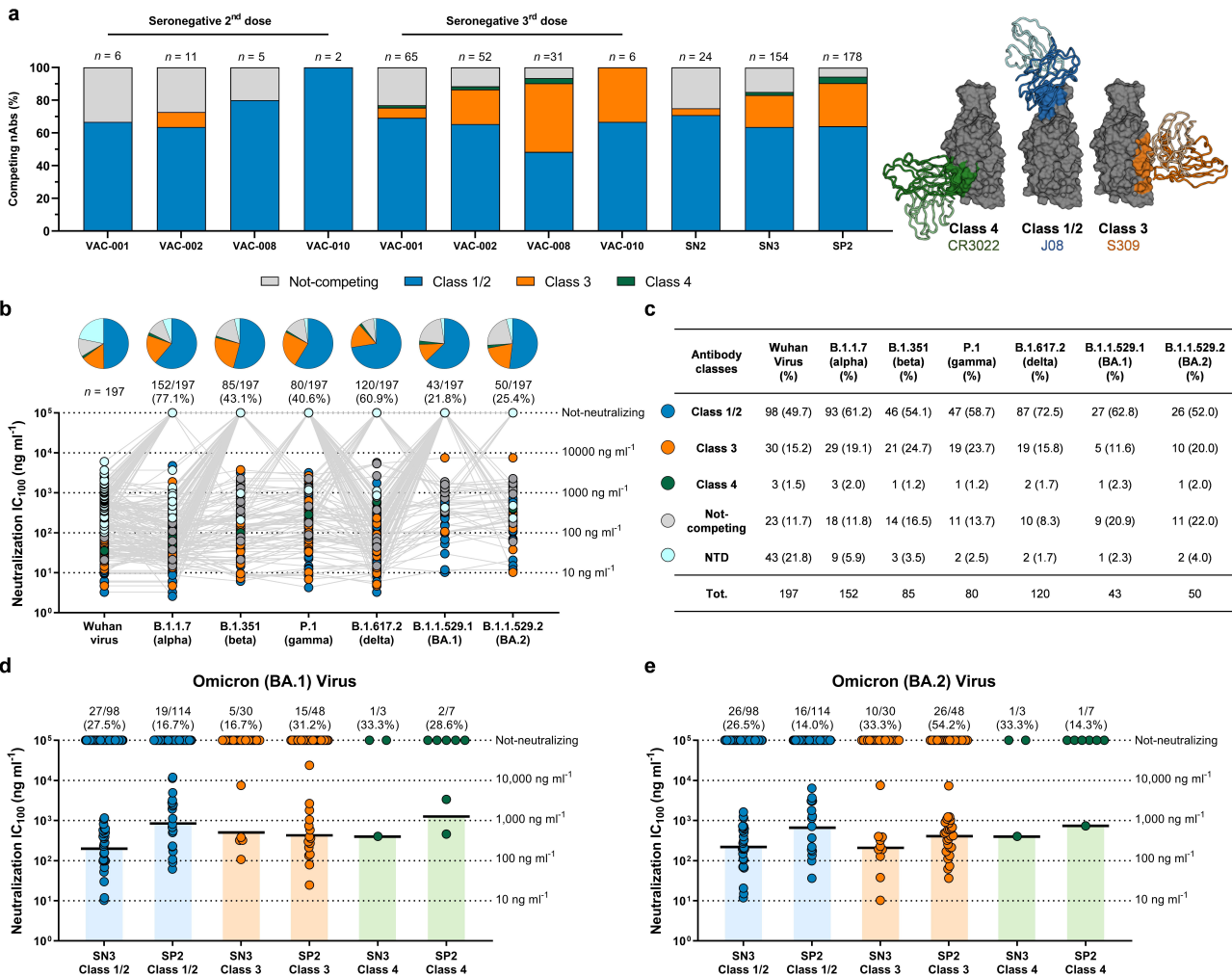
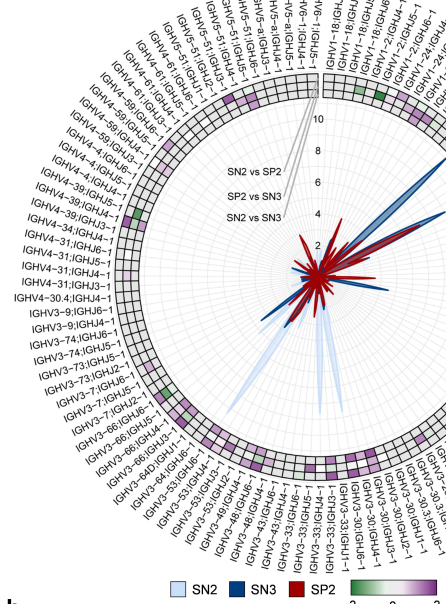
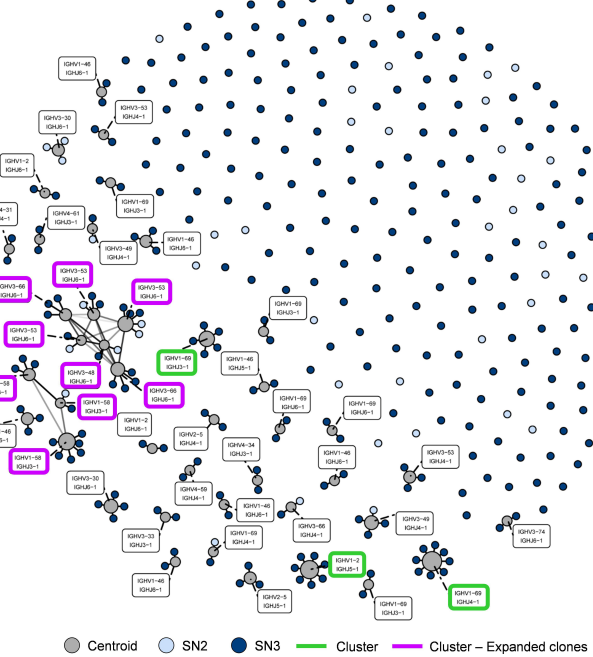


Figure 3

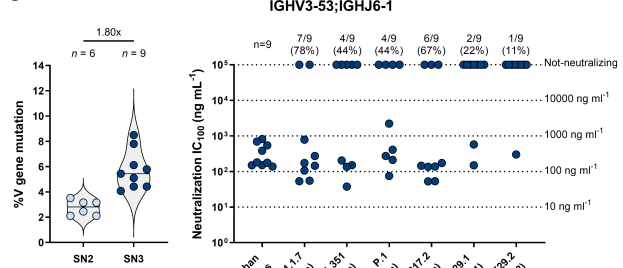
a



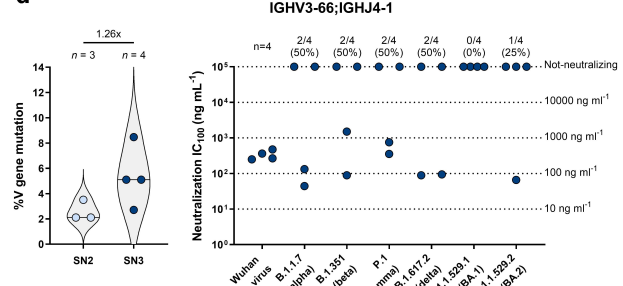
b



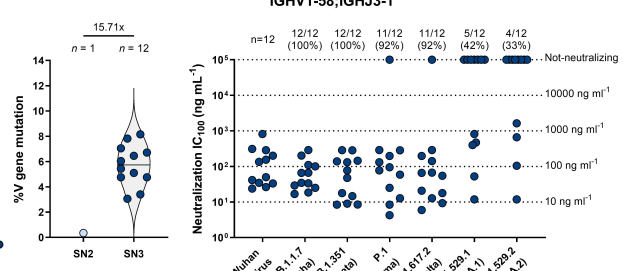
C



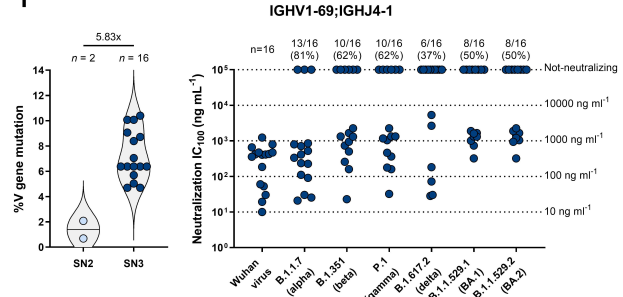
6



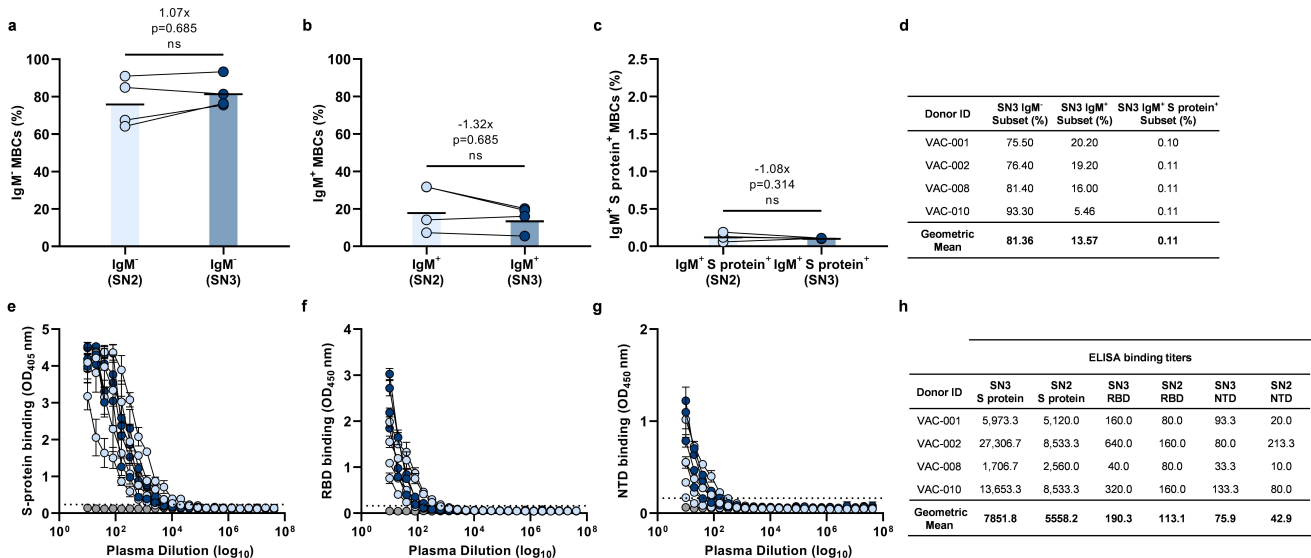
e



1

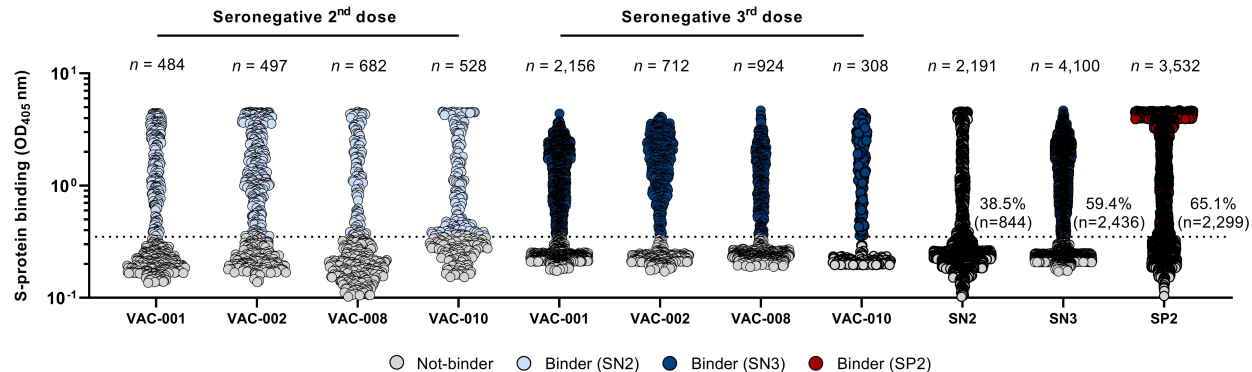


Extended Data Figure 1

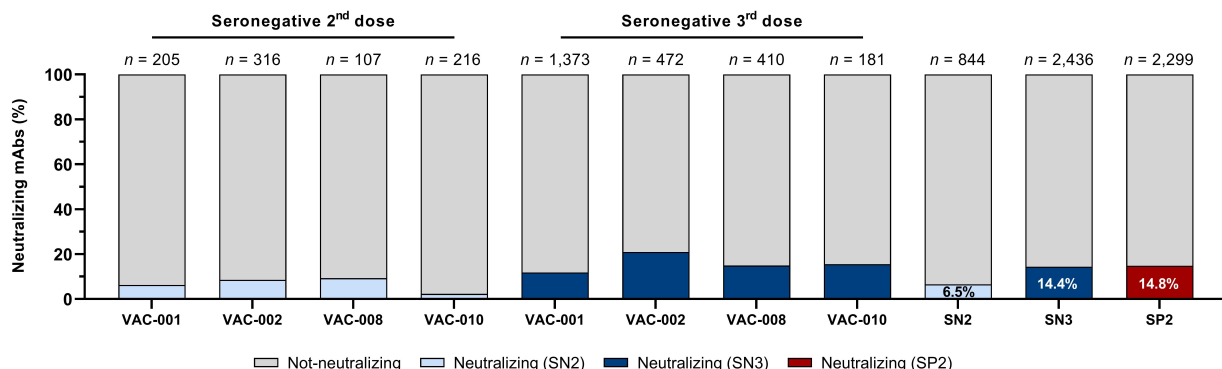


Extended Data Figure 2

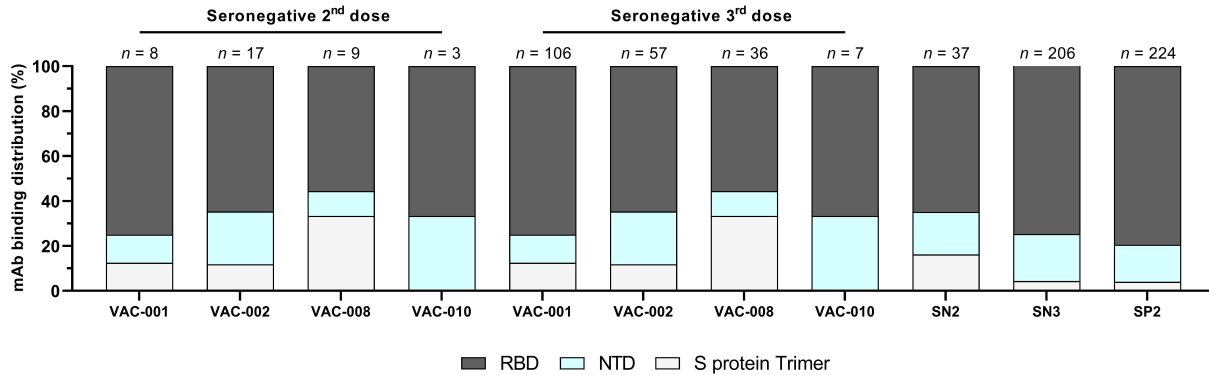
a



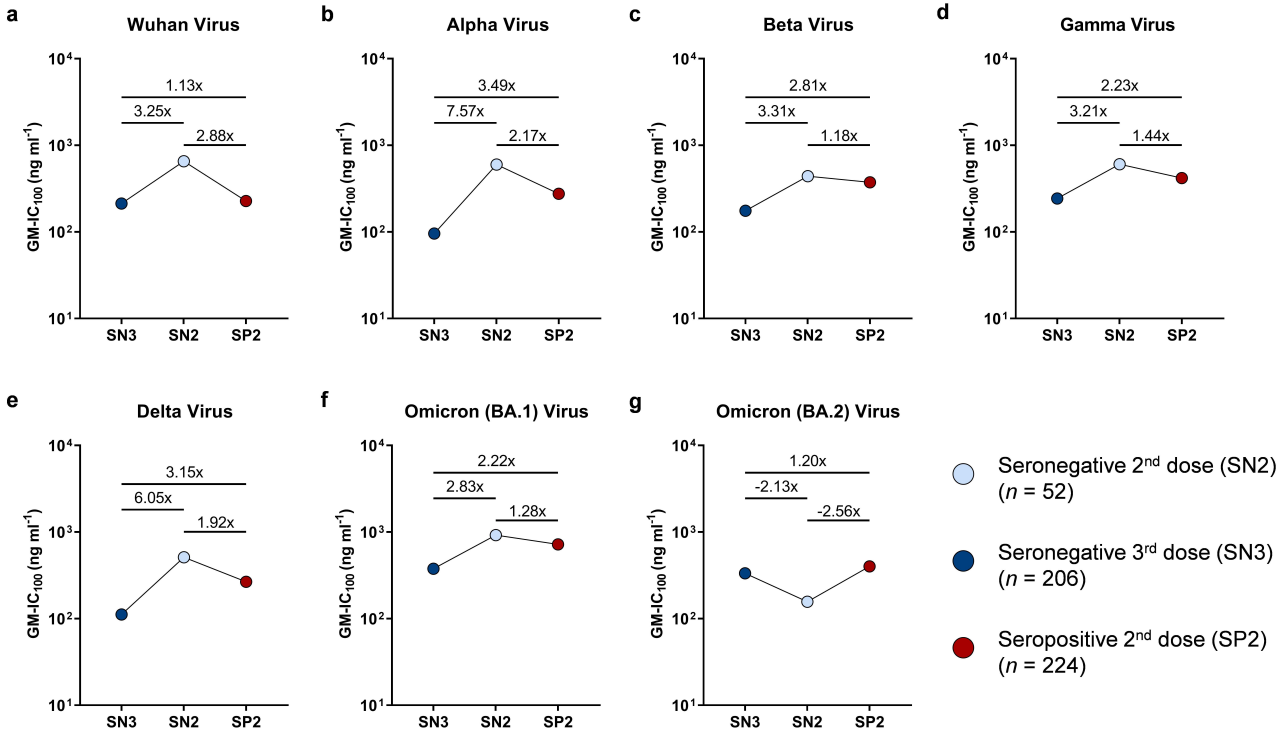
b



c

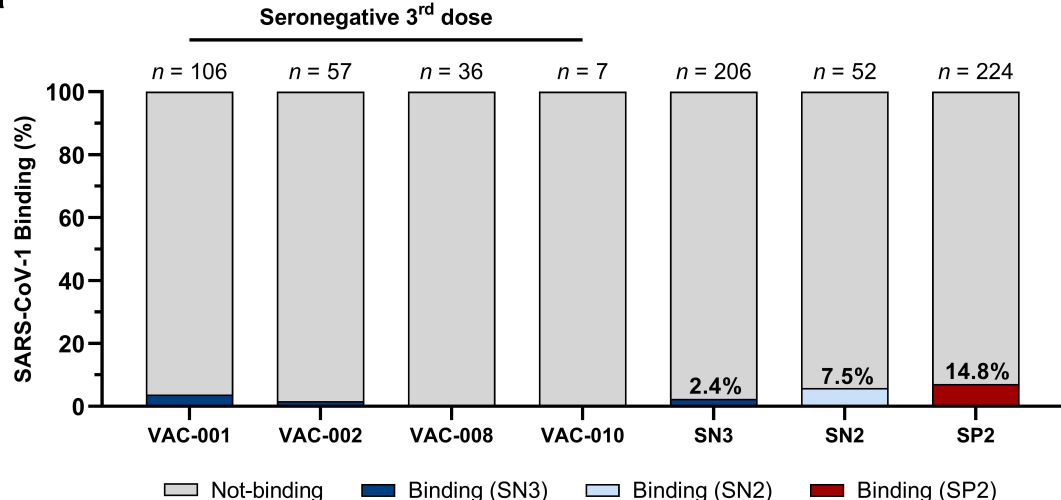


Extended Data Figure 3

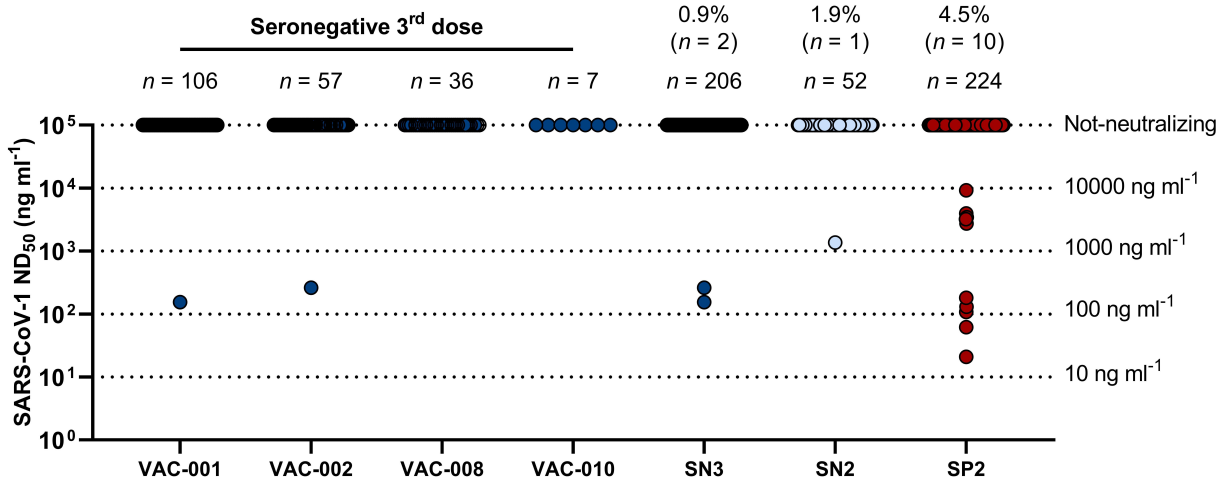


Extended Data Figure 4

a

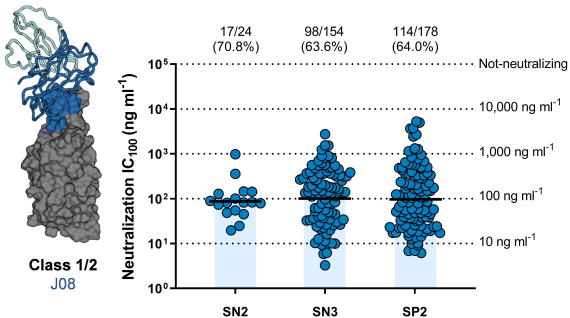


b



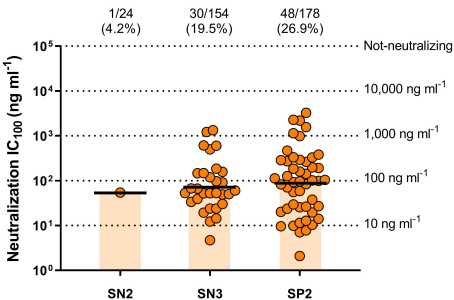
Extended Data Figure 5

a



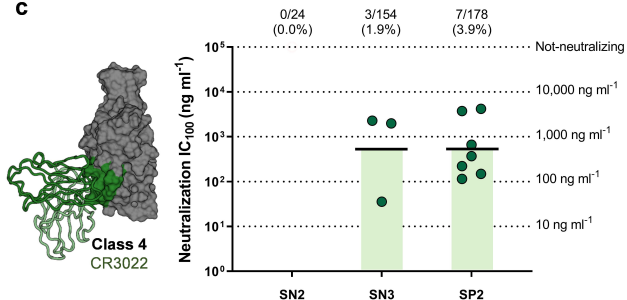
Class 1/2
J08

b



Class 3
S309

c

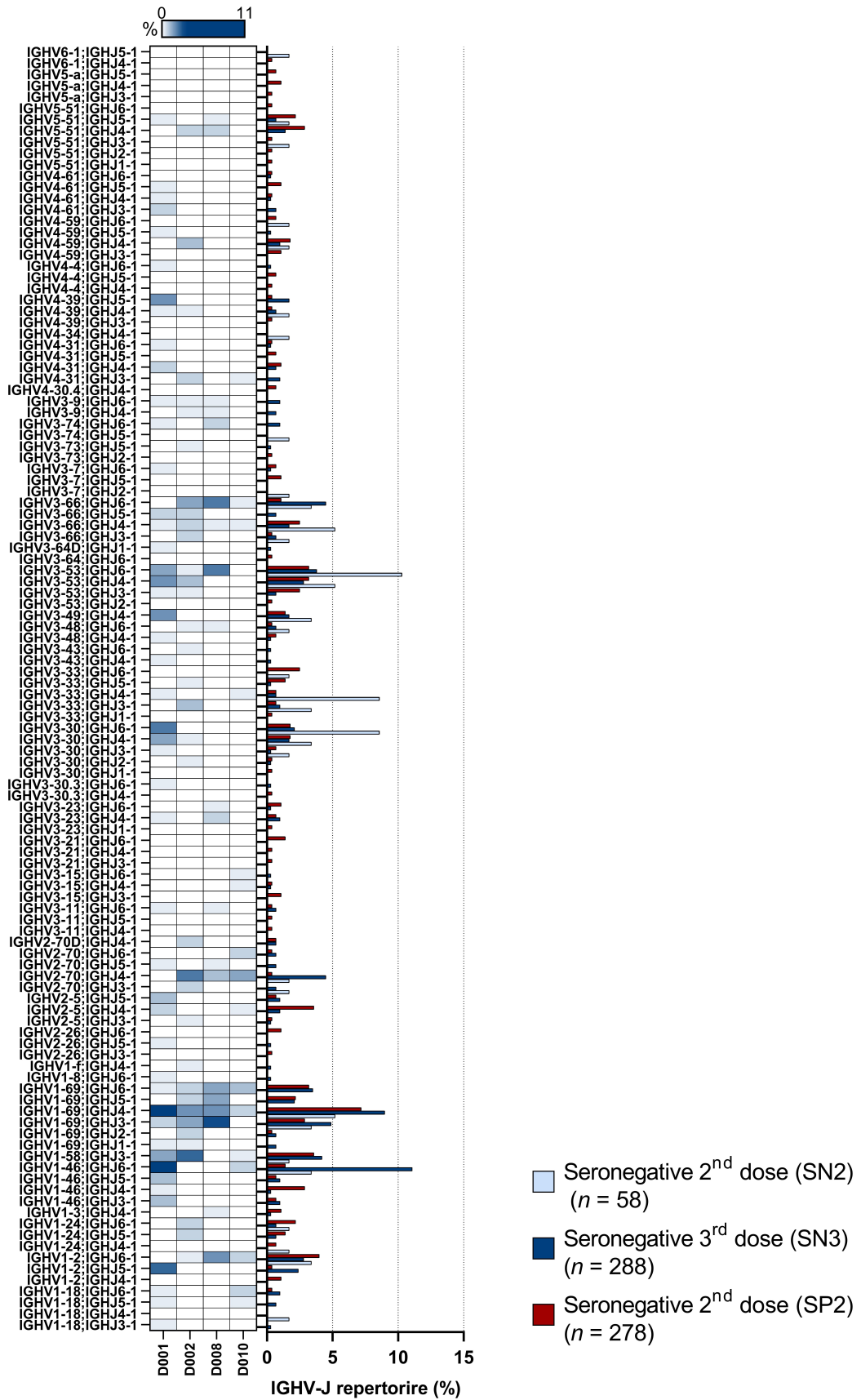


Class 4
CR3022

d

Cohort	Class 1/2	Class 3	Class 4
Seronegative 2 nd dose (SN2) GM-IC ₁₀₀ ng ml ⁻¹	89.5	54.0	N/A
Seronegative 3 rd dose (SN3) GM-IC ₁₀₀ ng ml ⁻¹	110.1	72.6	544.1
Seropositive 2 nd dose (SP2) GM-IC ₁₀₀ ng ml ⁻¹	109.5	89.5	545.9

Extended Data Figure 6



Extended Data Table 1

Subject ID	Gender	Age	First Dose (dd/mm/yy)	Second Dose (dd/mm/yy)	Third Dose (dd/mm/yy)	Vaccine	Days from Second to Third Dose	Blood Collection (dd/mm/yy)	Days from Third Dose to Blood Collection
VAC-001	M	39	27/12/2020	18/01/2021	28/10/2021	BNT162b2	283	13/01/2022	77
VAC-002	F	39	01/01/2021	22/01/2021	08/11/2021	BNT162b2	290	13/01/2022	66
VAC-008	M	44	03/01/2021	24/01/2021	23/11/2021	BNT162b2	303	12/01/2022	50
VAC-010	F	52	18/02/2021	11/03/2021	09/12/2021	mRNA-1273	277	20/01/2022	42

Extended Data Table 2

Subject	S protein ⁺ MBCs Sorted	S protein ⁺ mAbs (%)	Wuhan - Neutralizing antibodies (%)	Expressed - Neutralizing antibodies (%)	Expressed - Neutralizing antibodies (%) Alpha	Expressed - Neutralizing antibodies (%) Beta	Expressed - Neutralizing antibodies (%) Gamma	Expressed - Neutralizing antibodies (%) Delta	Expressed - Neutralizing antibodies (%) Omicron BA.1	Expressed - Neutralizing antibodies (%) Omicron BA.2
VAC-001	2,156	1,373 (63.7)	162 (11.8)	106 (65.4)	68 (64.2)	36 (34.0)	30 (28.3)	55 (51.9)	22 (20.8)	24 (22.6)
VAC-002	712	472 (66.3)	99 (21.0)	57 (57.6)	54 (94.7)	34 (59.6)	35 (61.4)	42 (73.7)	15 (26.3)	17 (29.8)
VAC-008	924	410 (44.4)	61 (14.9)	36 (59.0)	31 (86.1)	14 (38.9)	14 (38.9)	25 (69.4)	7 (19.4)	9 (25.0)
VAC-010	308	181 (58.8)	28 (15.5)	7 (25.0)	6 (85.7)	2 (28.6)	2 (28.6)	4 (57.1)	1 (14.3)	2 (28.6)
Total	4,100	2,436 (59.4)	350 (14.4)	206 (51.7)	159 (77.2)	86 (41.7)	81 (39.3)	126 (61.2)	45 (21.8)	52 (25.2)